2009 American Control Conference
Hyatt Regency Riverfront, St. Louis, MO, USA
June 10-12, 2009

Low-Order System Identification and Optimal Control of Intersample Behavior in ILC

Tom Oomen, Jeroen van de Wijdeven, and Okko Bosgra

Abstract— **Iterative Learning Control (ILC) enables high tracking performance of batch repetitive processes. Common ILC approaches resort to discrete time system representations and hence are not able to guarantee good intersample behavior in case the underlying system evolves in continuous time. The aim of this paper is to explicitly deal with the intersample behavior in ILC. A multirate, parametric, and low-order approach to both identification for ILC and subsequent optimal ILC is presented that results in a low computational burden. The approach appropriately deals with the time-varying nature of multirate systems. The proposed multirate identification and ILC algorithms are shown to outperform common ILC approaches in a simulation example.**

I. Introduction

Iterative Learning Control (ILC) is a control design strategy that enables high tracking performance of batch repetitive processes. Basically, ILC determines an optimal command signal based on measured signals from previous trials and limited plant knowledge. The resulting command signal can compensate for all trial-invariant signal components in the measured signals.

Commonly, ILC controllers for continuous time systems are implemented in a digital computer environment, as a result a sampled-data system is obtained. In this case, the ILC algorithm learns from *discretized* error signals and thus high *discrete time* performance is obtained. However, since the plant evolves in continuous time, it is more natural to evaluate performance in the continuous time domain.

In fact, pursuing high at-sample performance in sampled-data systems can go at the expense of a poor intersample behavior, see, e.g., [1], [2], [3] for sampled-data feedback control. In [4], [5], it is shown that ILC can also result in poor intersample behavior and *ad hoc* solutions are suggested. In [6], an optimal multirate ILC algorithm is presented that systematically deals with the intersample behavior.

Although the approach in [6] systematically deals with the intersample behavior, it resorts to plant models of different sampling frequencies that are not straightforward to obtain via LTI system identification techniques such as [7], [8]. In addition, similar to [9], [10], the optimal ILC algorithm in [6] involves Toeplitz matrices with dimensions depending on the trial length, sampling frequency ratio, and number of inputs and outputs. In this case, implementation of the algorithm is limited to short trial lengths, small sampling frequency ratios, and a small amount of inputs and outputs.

The authors are with the Eindhoven University of Technology, Eindhoven, The Netherlands, t.a.e.oomen@tue.nl, j.j.m.v.d.wijdeven@tue.nl, o.h.bosgra@tue.nl. This research is supported by Philips Applied Technologies, Eindhoven, The Netherlands.

In this paper, a parametric approach to ILC is considered that explicitly addresses the intersample behavior. Specifically, a parametric system identification approach for multirate ILC is presented that appropriately deals with the time varying nature of the multirate system. Subsequently, the identified model is used in optimal ILC, thereby explicitly accounting for the intersample behavior.

The presented optimal ILC algorithm exploits the low order of the parametric model. In contrast to [9] and [6], which resort to a linear least squares problem, the dimensions of the involved matrices in the proposed approach do not increase if the trial length, the sampling frequency ratio, or the number of inputs and outputs is increased. Specifically, a low-order solution is presented that requires solving one discrete time Riccati difference equation with dimensions equal to the state dimension of the parametric model. The proposed approach extends previous work, including [11], [12], by considering a more general criterion and by explicitly dealing with the intersample behavior. Thus, the presented approach enables an explicit treatment of the intersample behavior in ILC for multivariable systems with large trial lengths. As a special case, the procedure enables the design of low-order multivariable discrete time ILC controllers.

The paper is organized as follows. In Section II, the sampled-data ILC problem is formulated. In Section III, an approach is presented that enables system identification and optimal ILC for multirate systems, thereby appropriately dealing with the time-varying nature. Subsequently, Section IV and Section V deal with multirate identification and optimal ILC, respectively. In Section VI, an example is provided, which shows that the proposed multirate ILC algorithm outperforms common discrete time algorithms. Finally, conclusions are given in Section VII.

Notation. Throughout, $t \subseteq \mathbb{Z}$ and $t_c \subseteq \mathbb{R}$ denote discrete time and continuous time, respectively. To facilitate the notation, arguments are omitted if clear from the context. In block diagrams, solid lines represent continuous time signals, dashed lines represent slow sampled discrete time signals, and dotted lines represent fast sampled signals. It is assumed that sampling is non-pathological [6]. The forward shift operator is denoted by q. The delay operator D_τ is defined by $(D_\tau f)(t) = f(t-\tau)$, where $\tau \in t$. Systems are linear time invariant (LTI) if they commute with $D_\tau \ \forall \tau \in t$. The truncation operator is defined by $(P_\tau f)(t) = f(t)$ for $t \leq \tau$ and $(P_\tau f)(t) = 0$ for $t > \tau$. A system G is causal if $P_\tau G P_\tau = P_\tau G, \ \forall \tau \in t$. The discrete Fourier transform of a signal x is given by $X_N(\omega) = \frac{1}{\sqrt{N}} \sum_{t=1}^{N} x(t) e^{j\omega t}$. The notation $\|x\|_W$ denotes $x^T W x$, whereas $\|x\|_2$ denotes the standard 2-norm.

II. Problem formulation

A. Sampled-data setup

In this section, the ILC problem for closed-loop sampled-data systems is defined. The considered setup is depicted in Figure 1. Here, $y = Pu$, where P denotes the LTI continuous time plant with n_y outputs and n_u inputs. The plant input is given by

$$u = \mathcal{H}^h \mathcal{H}_u (w^l + C^{d,l} \mathcal{S}_d \mathcal{S}^h e) \tag{1}$$

$$e = r - y, \tag{2}$$

where r is the reference signal and $C^{d,l}$ is a discrete time internally stabilizing feedback controller operating at a sampling frequency f^l. In (1), the ideal sampler and zero-order-hold are defined by

$$\mathcal{S}^h : e(t_c) \mapsto e^h(t), e^h(t_i) = e(t_i h^h) \tag{3}$$

$$\mathcal{H}^h : u^h(t) \mapsto u(t_c), u(t_i h^h + \tau) = u^h(t_i),\ \tau = [0, h^h), \tag{4}$$

respectively, where $t_i \in t$, sampling frequency $f^h = \frac{1}{h^h}$, and h^h denotes the sampling time. In addition, the downsampling operator $\mathcal{S}_d$ is defined by

$$\mathcal{S}_d : e^h(t) \mapsto e^l(t),\ e^l(t_i) = e^h(F t_i), \quad t_i \in t, \tag{5}$$

where $F \in \mathbb{N}$ denotes the sampling frequency ratio, i.e., $f^h = F f^l$, where f^l is the sampling frequency at which $C^{d,l}$ operates. In addition, the multirate zero-order-hold $\mathcal{H}_u$ is defined as [2]

$$\mathcal{H}_u = \mathcal{I}^F(z) \mathcal{S}_u, \tag{6}$$

where the upsampler $\mathcal{S}_u$ and zero-order-hold interpolator $\mathcal{I}^F(z)$ are given by

$$\mathcal{S}_u : u^l(t) \mapsto x^h(t),\ x^h(t_i) := \begin{cases} u^l(\frac{t_i}{F}) & \text{for } \frac{t_i}{F} \in \mathbb{Z} \\ 0 & \text{for } \frac{t_i}{F} \notin \mathbb{Z}. \end{cases} \tag{7}$$

$$\mathcal{I}^F(z) = \textstyle\sum_{f=0}^{F-1} z^{-f}. \tag{8}$$

Note that the sampling at a high sampling frequency followed by downsampling can be replaced by sampling at a lower frequency, e.g., [6]. For the multirate ILC approach in Section II-B, however, the present formulation is convenient.

The main problem considered in this paper is given by the optimal sampled-data problem.

Definition 1 (Optimal sampled-data ILC): Given the criterion $\mathcal{J}_{\mathrm{SD}}(w^l, e)$, determine

$$w^l_{\mathrm{SD}^\star} = \arg\min_{w^l} \mathcal{J}_{\mathrm{SD}}(w^l, e). \tag{9}$$

In the optimal sampled-data ILC problem, an optimal *discrete time* command signal w^l is determined that achieves good *continuous time* performance e, see Figure 1. This implies that the problem involves both continuous time and discrete time signals. In contrast, standard ILC algorithms [13], [14], [15] employ discrete time measurements of the error e. In particular, the optimal discrete time ILC problem is given by the following definition.

Definition 2 (Optimal discrete time ILC): Given the criterion $\mathcal{J}_{\mathrm{DT}}(w^l, e^l)$, determine

$$w^l_{\mathrm{DT}^\star} = \arg\min_{w^l} \mathcal{J}_{\mathrm{DT}}(w^l, e^l). \tag{10}$$

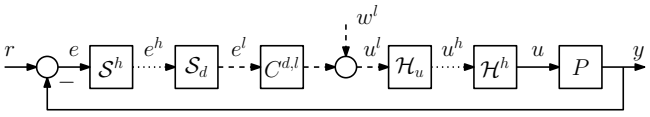

Fig. 1. Closed-loop multirate ILC setup.

In the discrete time ILC criterion $\mathcal{J}_{\mathrm{DT}}(w^l, e^l)$, only the at-sample response e^l is minimized, whereas the sampled-data criterion $\mathcal{J}_{\mathrm{SD}}(w^l, e)$ includes the intersample response. This implies that discrete time ILC approaches may result in poor intersample behavior, which is quantified by

$$\mathcal{J}_{\mathrm{SD}}(w^l_{\mathrm{DT}^\star}, e) \geq \mathcal{J}_{\mathrm{SD}}(w^l_{\mathrm{SD}^\star}, e). \tag{11}$$

In Section VI, it is illustrated that the gap in (11) can become arbitrarily large.

B. Towards a multirate approach

Since the continuous time error signal e can not be processed on a digital computer, a multirate approximation to the sampled-data ILC problem in Definition 1 is investigated to enable a digital computer implementation. The key idea is that in many applications, it is possible to measure error signals at a higher sampling frequency f^h than the frequency f^l at which $C^{d,l}$ operates. Indeed, the bound on f^l is often caused by the fact that in feedback control the new control input has to be computed in real-time. In contrast, although ILC is implemented in real-time, it can exploit the time in between trials for the actual computation of the command signal. This motivates the following multirate ILC problem.

Definition 3 (Optimal multirate ILC): Given the criterion $\mathcal{J}_{\mathrm{MR}}(w^l, e^h)$, determine

$$w^l_{\mathrm{MR}^\star} = \arg\min_{w^l} \mathcal{J}_{\mathrm{MR}}(w^l, e^h). \tag{12}$$

In [6], it is discussed that $w^l_{\mathrm{MR}^\star} \to w^l_{\mathrm{SD}^\star}$ for $h^h \to 0$. As in [6], the following criterion is considered, which is a multirate generalization of the criterion in [9], [10], etc.

Definition 4: The criterion for determining the optimal command input in trial $k+1$, i.e., $w^l_{<k+1>}$, is defined as

$$\mathcal{J}_{\mathrm{MR}<k+1>} = \tfrac{1}{2} \sum_{t=0}^{N^h-1} \left[\|e^h_{<k+1>}(t)\|_{W_e} \right] \tag{13}$$

$$+ \tfrac{1}{2} \sum_{t=0}^{N^l-1} \left[\|w^l{}_{<k+1>}(t)\|_{W_w} + \|w^l{}_{<k+1>}(t) - w^l{}_{<k>}(t)\|_{W_\Delta} \right],$$

where $N^h - 1$ and $N^l - 1$ are the trial lengths at the high and low sampling frequencies, respectively. Generally, optimal ILC solutions require some model knowledge of the mapping from the command signal to the error signal. In the multirate case, a model mapping w^l to e^h is required, i.e., assuming $r = 0$, then in

$$e^h = -J_{\mathrm{MR}} w^l \tag{14}$$

a model of J_{MR} is required. In [6], it is shown that J_{MR} is time-varying even if P in Figure 1 is time-invariant. Time-variance of J_{MR} can easily be understood if it is observed that e^h operates at a higher sampling frequency than w^l. In the next section, it is shown how to deal with the time varying nature of J_{MR} in view of system identification and subsequent multirate ILC control design.

Remark 5: The discrete time ILC case is recovered if $F = 1$, in which case the intersample behavior is discarded.

III. A TIME-INVARIANT AND NORM-EQUIVALENT REPRESENTATION OF A TIME-VARYING SYSTEM

In this section, a technical step is presented that enables system identification for multirate ILC and subsequent low-order optimal ILC. Throughout this section, the lifting operator has a central role in the derivations.

Definition 6: [16], [1] *The lifting operator $\mathcal{L}$, $\widetilde{e}^h = \mathcal{L}e^h$, is defined by*

$$\widetilde{e}(t_i) = \begin{bmatrix} e^h(Ft_i) \\ e^h(Ft_i+1) \\ \vdots \\ e^h(Ft_i+F-1) \end{bmatrix}. \tag{15}$$

In Definition 6, e^h is an n_y dimensional signal with sampling frequency f^h, whereas $\widetilde{e}^h$ is an Fn_y dimensional signal with sampling frequency f^l. The following proposition reveals that $\mathcal{L}$ preserves the 2-norm, which is useful in case a certain norm-based criterion is minimized.

Proposition 7: Consider the lifting operator $\mathcal{L}$ in Definition 6. Then, $\|\widetilde{e}\|_2 = \|e^h\|_2$.

Proof: Results from evaluating the vector 2-norm. ■

Next, causality of the lifting operator $\mathcal{L}$ is investigated.

Proposition 8: Consider the lifting operator $\mathcal{L}$ in Definition 6 and let $F > 1$. Then, $\mathcal{L}$ is not a causal operator.

Proof: Follows by considering the definition of causality for $\tau = 0$. ■

Proposition 8 reveals that the lifting operator $\mathcal{L}$ is not causal. Hence $\widetilde{e}$ is not available for feedback control, since in this case the controller has to operate in real-time based on past measurement data. In contrast, in Section IV and Section V it will be shown how the lifting operator can be exploited in system identification and optimal ILC, respectively.

Next, consider the setup in Figure 1. Here, $\mathcal{H}^h$ and $\mathcal{S}^h$ are absorbed in P to obtain $P^{d,h}$, which is an LTI system operating at sampling frequency h^h [6]. In this case, the time-varying mapping in (14) is given by

$$J_{\mathrm{MR}} = P^{d,h}\mathcal{H}_u(I + C^{d,l}P^{d,l})^{-1}. \tag{16}$$

The following proposition reveals that J_{MR} can be recast as an LTI mapping.

Proposition 9: Let $(A_p^h, B_p^h, C_p^h, D_p^h)$ be a minimal state-space realization of $P^{d,h}$, let $(A_c^l, B_c^l, C_c^l, D_c^l)$ be a minimal state-space realization for $C^{d,l}$, and assume that $D_p^h D_c^l = 0$, $D_c^l D_p^h = 0$. Then, a minimal state-space realization for $\mathcal{L}P^{d,h}\mathcal{H}_u(I + C^{d,l}P^{d,l})^{-1}$ is given by the state-space realization $(\widetilde{A}, \widetilde{B}, \widetilde{C}, \widetilde{D})$, i.e.,

$$\left[\begin{array}{cc|c} (A_p^h)^F - \mathfrak{B}D_c^l C_p^h & \mathfrak{B}C_c^l & \mathfrak{B} \\ -B_c^l C_p^h & A_c^l - B_c^l D_p^h C_c^l & -B_c^l D_p^h \\ \hline C_p^h & D_p^h C_c^l & D_p^h \\ C_p^h A_p^h - C_p^h B_p^h D_c^l C_p^h & D_p^h C_c^l + C_p^h B_p^h C_c^l & D_p^h + C_p^h B_p^h \\ \vdots & \vdots & \vdots \\ C_p^h (A_p^h)^{F-1} - \mathfrak{D}D_c^l C_p^h & \mathfrak{D}C_c^l & \mathfrak{D} \end{array}\right]$$

$$\mathfrak{B} = \sum_{f=0}^{F-1} (A_p^h)^f B_p^h, \quad \mathfrak{D} = D_p^h + \sum_{f=0}^{F-2} C_p^h (A_p^h)^f B_p^h.$$

The proof follows from extensive computations based on successive substitution and is omitted because of space limitations. The interpretation of $\widetilde{C}, \widetilde{D}$ is that the multirate system is in 'open-loop' in between the controller sampling instants. Proposition 9 leads to the following result that is required to enable application of system identification tools for finite dimensional LTI systems.

Proposition 10: The system $\mathcal{L}P^{d,h}\mathcal{H}_u(I + C^{d,l}P^{d,l})^{-1}$:

a) is LTI,

b) has McMillan degree upper bounded by the sum of the McMillan degrees of P and $C^{d,l}$

c) $\in \mathcal{RH}_\infty^{Fn_y \times n_u}$.

Proof: To show (a), observe that $D_\tau(\mathcal{L}P^{d,h}\mathcal{H}_u(I + C^{d,l}P^{d,l})^{-1}) = \mathcal{L}P^{d,h}\mathcal{H}_u(I+C^{d,l}P^{d,l})^{-1}D_\tau \ \forall \tau \in t$, hence the system is LTI. To show (b), note that the McMillan degree of a proper system equals the state dimension of a minimal state-space realization. Next, the state-space realization of the system in Proposition 9 has a McMillan which is equal to the sum of the McMillan degrees of $C^{d,l}$ and P, where the McMillan degree of P is invariant under (down)sampling, see [6]. Finally, inequality is obtained by possible nonminimality of $(\widetilde{A}, \widetilde{B}, \widetilde{C}, \widetilde{D})$, which can be caused by pole/zero cancellations between $C^{d,l}$ and $P^{d,l}$. Part (c) directly follows from the fact that $C^{d,l}$ is internally stabilizing, hence $\widetilde{A}$ is strictly Hurwitz and as a result $\mathcal{L}P^{d,h}\mathcal{H}_u(I+C^{d,l}P^{d,l})^{-1} \in \mathcal{RH}_\infty^{Fn_y \times n_u}$. ■

IV. SYSTEM IDENTIFICATION FOR MULTIRATE ILC

ILC requires a model of the true system. Especially in case of optimal ILC, as is considered in Section V, a higher model accuracy is required compared to less complex ILC approaches such as Arimoto-type of ILC controllers. A fast and inexpensive method to obtain such an accurate model for ILC is to employ system identification.

The multirate ILC problem, as discussed in Section II-B, requires a model J_{MR} that maps w^l to $-e^h$. The mapping J_{MR} is time-varying due to the different sampling frequencies of w^l and e^h, which obstructs a direct application system identification tools for LTI systems. Building on the developments in Section III, the system identification for multirate ILC problem is investigated in this section and a solution that enables use of standard LTI system identification approaches is presented.

To deal with the identification of $J_{\mathrm{MR}} : w^l \mapsto -e^h$, the lifting approach in Section III is exploited. Specifically, Proposition 9 and Proposition 10 imply that the operator J_{MR} can be appended with the lifting operator to obtain the LTI MIMO system $\widetilde{J_{\mathrm{MR}}} = \mathcal{L}J_{\mathrm{MR}} = \mathcal{L}P^{d,h}\mathcal{H}_u(I+C^{d,l}P^{d,l})^{-1}$. Thus, standard identification methods for multivariable LTI systems can be applied, e.g., [7], [8].

In case prediction error identification is pursued, then in virtue of the system relation, the model

$$\widetilde{y}^h(t) = -\widetilde{e}(t) = \widetilde{J_{\mathrm{MR}}}(q)w^l(t) + \widetilde{H}(q)v(t), \tag{17}$$

is postulated, where $\widetilde{H}(q)$ is a bistable LTI system and the reference $r(t) = 0$. Note that (17) involves a closed-loop setup. However, closed-loop operators are being estimated and hence essentially an open-loop system identification problem is obtained. Although $\widetilde{H}$ depends on $C^{d,l}$, e.g., [17], knowledge of $C^{d,l}$ is not required in the identification procedure. In this respect, the suggested approach closely resembles the indirect identification approach.

In case of a model of the form (17), the goal of prediction error identification is to minimize $\|\widetilde{\varepsilon}(t)\|_2^2$, where

$$\widetilde{\varepsilon}(t) = \widetilde{H}^{-1}(q)\left(-\widetilde{e}(t) - \widetilde{J_{\mathrm{MR}}}(q)w^l(t)\right), \qquad (18)$$

see [7] for details. Note that in virtue of Proposition 7, $\arg\min \|\varepsilon(t)\|_2^2 = \arg\min \|\mathcal{L}^{-1}\widetilde{\varepsilon}(t)\|_2^2$, hence the suggested approach minimizes the prediction error $\varepsilon(t)$ in the original, time varying setting.

Summarizing, the suggested identification procedure is as follows:

1) set $r = 0$ and apply a suitable input signal w^l,
2) measure $e^h(t) = -y^h(t)$,
3) lift the measured error signal, i.e., $\widetilde{e} = \mathcal{L}e^h(t)$,
4) identify the MIMO LTI system $\widetilde{J_{\mathrm{MR}}}$ that minimizes the prediction error $\widetilde{\varepsilon}$ in (18).

The parametric identification approach presented in this section has advantages over identification of a nonparametric FIR model, as is required for ILC algorithms such as [9]. In particular, since parametric models result in a smaller number of parameters, the parameter variance is typically reduced and the resulting model can be used more efficiently compared to nonparametric models, as is shown in Section V. However, the model order should be chosen sufficiently high to avoid bias errors [7].

In the next section, it is shown how the identified LTI model can be used to solve the multirate ILC problem.

V. Optimal multirate ILC

In this section, a solution to the multirate optimal ILC problem, see Definition 3, is presented by exploiting the lifting operator, see Section III. Firstly, it is shown how lifted signals can be used to obtain a criterion equivalent to (13).

Proposition 11: Consider the lifting operator in Definition (6) *and criterion* (13) *in Definition 4. Then,*

$$\mathcal{J}_{\mathrm{MR}<k+1>} = \tfrac{1}{2}\sum_{t=0}^{N^l-1}\Big[\|\widetilde{e}_{<k+1>}\|_{\widetilde{W}_e} + \|w^l{}_{<k+1>}\|_{W_w} + \|w^l{}_{<k+1>} - w^l{}_{<k>}\|_{W_\Delta}\Big], \qquad (19)$$

where $\widetilde{W}_e := I_F \otimes W_e$ and $\otimes$ denotes the Kronecker product.

Proposition 11 enables the use of the results of Section III and Section IV in optimal multirate ILC. Specifically, it enables the direct usage of the identified LTI model in Section IV to solve the multirate ILC problem, thereby explicitly addressing the intersample behavior. The solution to the multirate ILC problem via the lifting operator is the main result of this section and is given in the following proposition.

Proposition 12: Consider the criterion (19) *and model $\widetilde{J} = (\widetilde{A}, \widetilde{B}, \widetilde{C}, \widetilde{D})$. Then,*

$$w^l_{<k+1>}(t) = C^{\mathrm{ILC}}\begin{bmatrix}\widetilde{e}_{<k>}(t)\\ w^l_{<k>}(t)\\ g_{<k>}(t+1)\end{bmatrix}, \qquad (20)$$

where C^{ILC} is given by the state-space realization

$$C^{\mathrm{ILC}} = \left[\begin{array}{c|ccc}\widetilde{A} - \widetilde{B}L(t) & \widetilde{B}L_e(t) & -\widetilde{B}L_w(t) & \widetilde{B}L_g(t)\\ \hline -L(t) & L_e(t) & I - L_w(t) & L_g(t)\end{array}\right]$$

$$L(t) = \Gamma_2^{-1}(\widetilde{B}^T P(t+1)A + \widetilde{D}W_e\widetilde{C})$$
$$L_e(t) = \Gamma_2^{-1}\widetilde{D}^T W_e, \quad L_w(t) = \Gamma_2^{-1}W_w, \quad L_g(t) = \Gamma_2^{-1}\widetilde{B}^T$$
$$\Gamma_1 = W_w + W_\Delta + \widetilde{D}^T W_e \widetilde{D}, \quad \Gamma_2 = \Gamma_1 + \widetilde{B}^T P(t+1)\widetilde{B},$$

and P and $g_{<k>}$ are given by the backward recursions

$$P(t) = H_{21} + H_{22}P(t+1)(I - H_{12}P(t+1))^{-1}H_{11} \qquad (21)$$

$$\begin{aligned} g_{<k>}(t) = {} & \qquad (22)\\ & (H_{22} + H_{22}P(t+1)(I - H_{12}P(t+1))^{-1}H_{12})g_{<k>}(t+1)\\ & - (E_{21} + H_{22}P(t+1)(I - H_{12}P(t+1))^{-1}E_{11}\widetilde{e}_{<k>}(t)\\ & - (E_{22} + H_{22}P(t+1)(I - H_{12}P(t+1))^{-1}E_{12}w^l_{<k>}(t), \end{aligned}$$

where $P(N^l) = 0$, $g_{<k>}(N^l) = 0$, and

$$H = \left[\begin{array}{c|c}\widetilde{A} - \widetilde{B}\Gamma_1^{-1}\widetilde{D}^T\widetilde{W}_e\widetilde{C} & -\widetilde{B}\Gamma_1^{-1}\widetilde{B}^T\\ \hline \widetilde{C}^T\widetilde{W}_e\widetilde{C} - \widetilde{C}^T\widetilde{W}_e\widetilde{D}\Gamma_1^{-1}\widetilde{D}^T\widetilde{W}_e\widetilde{C} & \widetilde{A}^T - \widetilde{C}^T\widetilde{W}_e\widetilde{D}\Gamma_1^{-1}\widetilde{B}^T\end{array}\right]$$

$$E = \left[\begin{array}{c|c}\widetilde{B}\Gamma_1^{-1}\widetilde{D}^T\widetilde{W}_e & -\widetilde{B}\Gamma_1^{-1}W_w\\ \hline -\widetilde{C}^T\widetilde{W}_e + \widetilde{C}^T W_e\widetilde{D}\Gamma_1^{-1}\widetilde{D}^T\widetilde{W}_e & -\widetilde{C}^T\widetilde{W}_e\widetilde{D}\Gamma_1^{-1}W_w\end{array}\right]$$

A proof of Proposition is omitted due to space limitations. The proof is closely related to the solution of the linear quadratic tracking problem, e.g., [18, Chapter 4]. The derivation is significantly more involved due to the more complex criterion (19) and the presence of a direct feedthrough $\widetilde{D}$ in the multirate case.

Remarks:

- The solution to the linear quadratic tracking problem is known to be not causal, since the future reference signal is required in the optimization. In the ILC problem, the error $\widetilde{e}_{<k>}$ and command signal $w^l_{<k>}$ from the previous trial constitute the reference signal, resulting in a causal control law in the trial domain, yet a non-causal control law in the physical time domain.
- In analogy to the solution to the finite time linear quadratic optimal control problem [18], the controller C^{ILC} is time-varying. This results from the solution method to the two-point boundary-value problem. Alternatively, a time-invariant result can be derived, followed by an appropriate selection of boundary conditions, as is suggested in [19] for the finite time LQ problem.
- In contrast to the implementation of the linear quadratic optimal controller, the ILC controller does not require full state measurement or a state observer [18]. Instead, the optimal command signal $w^l_{<k+1>}$ is computed based on the computed optimal state trajectory, *before* trial $k+1$ is started. Inclusion of a state measurement or an observer during trial $k+1$ would lead to current-iteration ILC [14].
- The main computational burden in the implementation of the results of Proposition 12 are solution of a discrete time Riccati equation (21) and backward recursion (22), as well as the filtering by the time varying controller C^{ILC}, both involving matrices of size equal to the state dimension of the (low-order) model $\widetilde{J_{\mathrm{MR}}}$. In this respect, increasing the trial length N^l, sampling ratio factor F, or the number of inputs and outputs of P only affects the length of the signals to be filtered. This does not seriously obstruct numerical implementation. In contrast, the approach in [6], [9], [10] resorts to a linear least squares problem that involves matrices whose dimensions scale with N^l. In this case, solutions will only be feasible for limited values of N^l, F, n_u, and n_y.

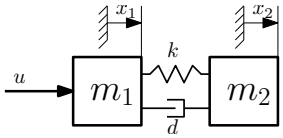

Fig. 2. Mechanical system.

VI. Example

A. Description

The mechanical system in Figure 2 is considered. Considering input u and output $y = \frac{d}{dt}x_1$, a state-space realization of the true system is given by

$$P_o = \left[\begin{array}{ccc|c} -\frac{d}{m_1} & \frac{d}{m_1} & \frac{k}{m_1} & \frac{1}{m_1} \\ \frac{d}{m_2} & -\frac{d}{m_1} & -\frac{k}{m_2} & 0 \\ -1 & 1 & 0 & 0 \\ \hline 1 & 0 & 0 & 0 \end{array}\right], \qquad (23)$$

the corresponding state vector is given by $x = \left[\frac{d}{dt}x_1 \quad \frac{d}{dt}x_2 \quad x_2 - x_1\right]$. In addition, $m_1 = m_2 = 4.8 \cdot 10^{-6}$, $k = 0.22$, and $d = 1 \cdot 10^{-4}$. A stabilizing feedback controller is given by the state-space realization

$$C^{d,l} = \left[\begin{array}{c|c} 0.6859 & 0.0132 \\ \hline 0.0132 & 10^{-4} \end{array}\right], \qquad (24)$$

which is implemented with a sampling frequency $f^l = 500$ Hz, i.e., $h^l = 2 \cdot 10^{-2}$. In addition, it is possible to measure the error signal with a sampling frequency $f^h = 1500$ Hz, hence $F = 3$.

B. Example 1: System identification

In this section, the system identification results of Section IV are illustrated. The setup in Figure 1 is considered, where $r = 0$. Multivariable prediction error identification is performed, see, e.g., [7], [20].

The input w^l is a normally distributed zero-mean white noise signal with variance 1. The output e^h is measured and is contaminated by noise, i.e.,

$$e^h = -P^{d,h}\mathcal{H}_u(I + C^{d,l}P^{d,l})^{-1}w^l + v, \qquad (25)$$

where v is a normally distributed zero-mean white noise signal with variance $2.5 \cdot 10^3$. A total measurement time of 0.2 s is used for identification purposes. Note that w^l is sampled with sampling frequency f^l, whereas e^h is sampled with sampling frequency f^h.

To enable usage of standard identification approaches, the signal e^h is lifted such that the mapping $w^l \mapsto \widetilde{e}^h$ is a finite dimensional LTI SIMO system. An output-error model is identified that minimizes the quadratic prediction error $\|\widetilde{\varepsilon}\|_2^2$. The reason for considering an output-error model structure is twofold. Firstly, a consistency result for independently parameterized disturbance models, including output-error models, is available in the situation of an incorrectly identified disturbance model. Secondly, (25) exactly corresponds to the output-error model structure.

To illustrate the results of Proposition 10, models of various orders are identified and subsequently validated using independent validation data. In Figure 3, the corresponding trace of the covariance matrix of the prediction error $\mathrm{tr}(C_\varepsilon)$,

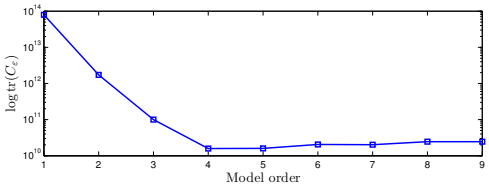

Fig. 3. Example 1: validation results.

which is a commonly used criterion [7], [20], is depicted for various model errors. For model order 1 up to 3, there is a large error due to undermodelling. Model order 4, which is the theoretically correct value, see Proposition 10, results in the smallest value. For model orders 5 and higher, the prediction error increases due to the fact that noise is modeled as input-output data due to an overparametrization and independent validation data is used, see also [7].

C. Example 2: Iterative learning control

Using the identified fourth order model, the multirate ILC approach of Section V is applied. To illustrate superiority of the proposed multirate techniques over present discrete ILC algorithms, the approach is applied for both $F = 3$ and $F = 1$, the former corresponds to the multirate case, whereas in the latter case the discrete time case is recovered. The ILC trial length $N^l = 8$, hence $N^h = 24$. A short trial length is chosen since this enables a clear exposition of the results, the approach is also feasible for longer trial lengths. Throughout this section, $W_e = 1$, $W_w = 0$, $W_\Delta = 10^{-6}$.

The initial sampled tracking error $e_{<0>}$ is depicted in Figure 4 (a) and Figure 5 (a). In Figure 4, the tracking error in the time domain is shown at both sampling frequencies f^l and f^h. In Figure 5, the cumulative normalized periodogram is depicted. The normalized periodogram of a discrete time signal $x(t)$, $t \in [0, N-1]$, is defined as

$$\Psi(\omega) = \frac{1}{N}|X_N(\omega)|^2. \qquad (26)$$

The periodogram is a useful measure for investigating the distribution of power of a signal over frequency. The normalization in (26) is useful for comparing signals of different sampling frequencies.

Analysis of the initial tracking error $e_{<0>}$ at sampling frequency f^h reveals that the error contains two dominant frequency components at 125 Hz and 437.5 Hz. At the sampling frequency f^l, the 437.5 Hz component appears as an aliased component at 62.5 Hz.

Firstly, the error signal $e^l_{<0>}(t)$ is used in the discrete time ILC control law, i.e., $F = 1$ and hence the intersample behavior is discarded. The error after 20 iterations $e_{\mathrm{DT}<20>}$ at both sampling frequency f^l and f^h is depicted in Figure 4 (b) and Figure 5 (b). It can be observed that at the sampling frequency f^l, the ILC controller performs a perfect task, since $e^l_{\mathrm{DT}<20>} = 0$. However, when investigating the intersample response, it can be observed that the converged error $e^h_{\mathrm{DT}<20>}$ has deteriorated compared to $e^h_{\mathrm{DT}<0>}$, i.e., the ILC controller results in performance deterioration of the sampled-data system. Analysis of Figure 5 (b) reveals that the ILC controller has effectively attenuated the 125 Hz frequency component. At sampling frequency f^h, a 62.5 Hz

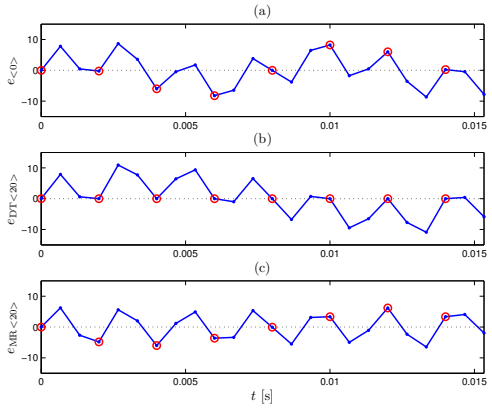

Fig. 4. Example 2: Comparison of error signals at sampling frequencies f^h (dots) and f^l (circles).

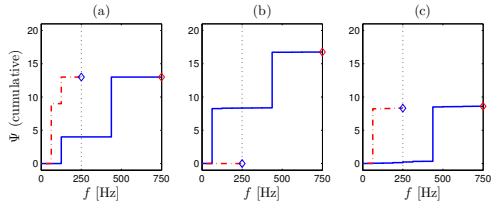

Fig. 5. Example 2: Comparison of error signals at sampling frequencies f^h (solid) and f^l (dash-dotted).

component has appeared, which in conjunction with the 437.5 Hz component results in poor intersample behavior.

Next, the error signal $e^h_{<0>}(t)$ is used in the multirate ILC control law of Section V, where $F = 3$. The error after 20 iterations $e_{\mathrm{MR}<20>}$ at both sampling frequency f^l and f^h is depicted in Figure 4 (c) and Figure 5 (c). It is concluded that the multirate ILC controller effectively attenuates the 125 Hz frequency component. However, it does not attempt to attenuate the 437.5 Hz component. As a result, this component is still present after convergence at sampling frequency f^h and at sampling frequency f^l as an aliased component. Clearly, this component cannot be attenuated using w^l.

The results in Figure 4 and Figure 5 are confirmed by the value of the criterion $\mathcal{J}_{\mathrm{MR}}$. Specifically, in the initial situation, $\mathcal{J}_{\mathrm{MR}}(w^l_{<0>}, e^h_{<0>}) = 624$. After convergence of the discrete time and multirate ILC algorithms, the results become $\mathcal{J}_{\mathrm{MR}}(w^l_{\mathrm{DT}<20>}, e^h_{\mathrm{DT}<20>}) = 804$ and $\mathcal{J}_{\mathrm{MR}}(w^l_{\mathrm{MR}<20>}, e^h_{\mathrm{MR}<20>}) = 413$, respectively.

Concluding, although discrete time ILC results in a perfect tracking error at sampling frequency f^l, it results in poor intersample behavior. In contrast, multirate ILC improves the true performance of the system by appropriately balancing the at-sample error and intersample responses.

VII. Conclusions

In this paper, a low-order optimal ILC approach has been presented that explicitly accounts for the intersample behavior in sampled-data systems. The approach is multirate and hence time-varying.

System identification for ILC has been discussed and the time-varying nature of the multirate system has been appropriately dealt with. It has also been established that system identification techniques for LTI systems can be used for multirate systems and low-order parameterizations have been presented.

A low-order optimal ILC controller is presented that resorts to the identified model and explicitly addresses the intersample response. Compared to impulse-response based optimal ILC controllers, which are computationally intractable for large trial lengths N^l, large sampling frequency ratios F, and multivariable systems with many inputs and outputs, the low-order ILC approach enables application of ILC to large-scale systems.

Simulation results confirm that system identification can deliver low-order parametric models that are suitable for optimal ILC. Comparing the proposed approach with standard approaches reveals that discrete time ILC can result in a poor intersample behavior, whereas the proposed multirate ILC controller significantly outperforms by appropriately balancing the at-sample response and the intersample behavior.

References

[1] T. Chen and B. Francis, *Optimal Sampled-Data Control Systems*. London, UK: Springer, 1995.

[2] T. Oomen, M. van de Wal, and O. Bosgra, "Design framework for high-performance optimal sampled-data control with application to a wafer stage," *Int. J. Contr.*, vol. 80, no. 6, pp. 919 – 934, 2007.

[3] M. M. Seron, J. H. Braslavsky, and G. C. Goodwin, *Fundamental Limitations in Filtering and Control*. London, UK: Springer-Verlag, 1997.

[4] R. W. Longman and C.-P. Lo, "Generalized holds, ripple attenuation, and tracking additional outputs in learning control," *J. Guid., Contr., Dyn.*, vol. 20, no. 6, pp. 1207–1214, 1997.

[5] P. A. LeVoci and R. W. Longman, "Intersample error in discrete time learning and repetitive control," in *Proc. AIAA/AAS Astrodynamics Specialist Conf. and Exhibit*, Providence, RI, USA, 2004, pp. 1–24.

[6] T. Oomen, J. van de Wijdeven, and O. Bosgra, "Suppressing intersample behavior in iterative learning control," *Automatica*, 2009, to appear, doi:10.1016/j.automatica.2008.10.022.

[7] L. Ljung, *System Identification: Theory for the User*, 2nd ed. Upper Saddle River, NJ, USA: Prentice Hall, 1999.

[8] R. Pintelon and J. Schoukens, *System Identification: A Frequency Domain Approach*. New York, NY, USA: IEEE Press, 2001.

[9] S. Gunnarsson and M. Norrlöf, "On the design of ILC algorithms using optimization," *Automatica*, vol. 37, pp. 2011–2016, 2001.

[10] J. van de Wijdeven and O. Bosgra, "Residual vibration suppression using Hankel iterative learning control," *Int. J. Rob. Nonlin. Contr.*, vol. 18, no. 10, pp. 1034–1051, 2008.

[11] B. G. Dijkstra and O. H. Bosgra, "Extrapolation of optimal lifted system ILC solution, with application to a waferstage," in *Proc. 2002 Americ. Contr. Conf.*, Anchorage, AK, USA, 2002, pp. 2595–2600.

[12] N. Amann, D. H. Owens, and E. Rogers, "Iterative learning control for discrete-time systems with exponential rate of convergence," *IEE Proc.-Control Theory Appl.*, vol. 143, no. 2, pp. 217–224, 1996.

[13] K. L. Moore, "Iterative learning control - an expository overview," *Appl. Comp. Contr. Sign. Proc. Circ.*, vol. 1, pp. 151–214, 1999.

[14] D. A. Bristow, M. Tharayil, and A. G. Alleyne, "A survey of iterative learning control: A learning-based method for high-performance tracking control," *IEEE Contr. Syst. Mag.*, vol. 26, no. 3, pp. 96–114, 2006.

[15] D. Gorinevsky, "Loop shaping for iterative control of batch processes," *IEEE Contr. Syst. Mag.*, vol. 22, no. 6, pp. 55–65, 2002.

[16] G. M. Kranc, "Input-output analysis of multirate feedback systems," *IRE Trans. Automat. Contr.*, vol. 3, no. 1, pp. 21–28, 1957.

[17] P. M. J. Van den Hof, "Closed-loop issues in system identification," *Annual Reviews in Control*, vol. 22, pp. 173–186, 1998.

[18] F. L. Lewis and V. L. Syrmos, *Optimal Control*, 2nd ed. New York, NY, USA: John Wiley & Sons, Inc., 1995.

[19] E. Zattoni, "Structural invariant subspaces of singular Hamiltonian systems and nonrecursive solutions of finite-horizon optimal control problems," *IEEE Trans. Automat. Contr.*, vol. 53, no. 5, pp. 1279–1284, 2008.

[20] L. Ljung, *System Identification Toolbox™ User's Guide*, 7th ed. Natick, MA, USA: The Mathworks, Inc., 2008.